Biomed Microdevices (2008) 10:671–679
DOI 10.1007/s10544-008-9178-3

A flexible polymer tube lab-chip integrated with microsensors for smart microcatheter

Chunyan Li · Pei-Ming Wu · Jungyoup Han · Chong H. Ahn

Published online: 16 May 2008

Abstract A flexible polymer tube lab-chip integrated with physical and biochemical sensor modules mounted on a flexible spiral structure for measuring physiological (temperature/flow rate) and metabolic data (glucose concentration) in a catheter application was designed, fabricated and characterized in this work. This new approach not only provides a unique way to assemble multiple sensors on both the inside and outside the flexible polymer tube using standard microfabrication methods while avoiding wiring and assembling problems associated with previous methods, but also maintains catheter inherent lumen potency for in situ drug delivery or insertion of medical tools. Three well-known sensors: temperature sensor (RTD), flow rate sensor (hot film anemometry) and glucose biosensor (amperometric sensor) have been successfully fabricated and fully integrated outside the spirally rolled polymer tube (ID=500 μm, OD=650 μm) of this demonstration device. The fabricated sensors showed good performances not only in a planar configuration but also in a spirally rolled configuration. This flexible micro tube lab-chip system provides a generic platform for developing patient-specific "smart" microcatheters that incorporate microsensors, microactuators, microfluidic devices and wireless signal communication modules that are tailored for the patients' unique condition.

Keywords Flexible polymer tube lab-chip · Microcatheter · Glucose biosensor · Flow sensor · Temperature sensor

C. Li (✉) · P.-M. Wu · J. Han · C. H. Ahn
Microsystems and BioMEMS Laboratory,
Department of Electrical & Computer Engineering,
University of Cincinnati,
814 Rhodes Hall,
Cincinnati, OH 45221-0030, USA
e-mail: leecc@ececs.uc.edu

1 Introduction

Minimally invasive interventions enable diagnosis and treatment of many conditions and surgery to be performed through a small incision. Catheters are used in a variety of medical procedures where access is limited, and they create a channel for the passage of fluid or the entry of a medical device without the need for large surgical incisions. This approach greatly reduces the damage to healthy tissue, reducing recovery time and chance of infection. However, while catheterization only involves a small incision; the surgeon is deprived of the sensory feedback that is possible through large incisions. Furthermore, small catheter incision ports limit the size of the device that may be inserted, thereby limiting the ability to use larger artificial sensory systems. Miniaturized sensors can provide both precise information about location and biochemical diagnostic information to improve the efficiency of operations and open new possibilities to treat more medical problems using catheterization (French et al. 2003; Haga and Esashi 2004; Li et al. 2005a, b; Goosen 2002). For optimal diagnosis and treatment, many of the parameters need to be measured and normally these parameters are strongly linked to therapeutic outcome. Therefore, in many cases, it is useful to be able to perform different simultaneous measurements at the same location and it is preferable to assemble multiple sensors on a single catheter (Goosen et al. 1999; Goosen and French 1999; Goosen et al. 2000).

In the development of functional microcatheters, wiring, assembly, and packaging processes have been regarded as some of the most challenging tasks due to their high complexity and manufacturing cost. Microsensors are excellent candidates for integration into the catheter, especially due to their small dimensions; however, they have proven difficult to mechanically integrate into the

relatively soft material of most catheters. Most catheters are used only once to avoid a risk of transmitting disease between patients, so the price must be low to accommodate a disposable platform. The matter is further complicated if many sensors are needed on a single device. Currently available micromachining technologies are mostly focusing on the surface process; hence the available platform to fabricate and assemble multiple MEMS devices is based on in-plane structure. Accordingly, a review of various packaging methods for catheter application indicates that the most popular packaging method has involved first fabricating the microsensors on the rigid substrate (silicon, glass, plastic, etc.) and then incorporating these sensors into commercially available catheters by wire-bonding the sensors to a printed circuit board (Goosen 2002; Goosen et al. 1999; Goosen and French 1999; Goosen et al. 2000), polymer flip-chip bonding on the flexible substrate (Li et al. 2005a, b) or electroplating sensor electrodes onto micro wires fabricated by laser micromachining (Nakagawa et al. 1995). Another popular method involves complex and high cost 3D microfabrication techniques that include mechanical turning, excimer laser drilling, mechanical molding and so on (Mirtaheri et al. 2004). These previously described packaging methods (Goosen 2002; Goosen et al. 1999; Goosen and French 1999; Goosen et al. 2000) encounter difficulty in maintaining catheter lumen potency for therapeutic infusion or inserting guide wires because they include many insulated wires that access the sensors via the lumen. Many wires passing through the catheter lumen also resulted in low catheter flexibility. Even when wiring problems were solved (Li et al. 2005a, b; Nakagawa et al. 1995), handling, inserting and aligning small dimension packages into the round catheter was prohibitively labor intensive and challenging work. Finally, the catheters with multiple integrated sensors add even greater complexity, can result in excessive costs and affect the flow profile of blood.

Considering the difficulties associated with previous approaches for developing functional catheters, in our previous work (Li et al. 2007), we successfully fabricated glucose biosensors on the flexible Kapton film and then spirally rolled it into different diameter tubes. It demonstrated the potential for developing a novel flexible tube-type platform for catheter application and assembling different required MEMS components as proof of concept. This spirally rolled flexible polymer tube-type platform can be easily assembled at the tip of commercial catheters due to the structural affinity or work as a free-standing catheter. In this work, we propose a new flexible polymer tube lab-chip integrated with multiple microsensors on the tube wall for a smart microcatheter. This new fabrication and packaging method enables sensors, actuators, wires and circuits to be fabricated first on flexible polymer substrates using standard microfabrication techniques followed by spirally rolling the flexible substrate to form a 3D tube with microsensors inside and/or outside the polymer tube. Figure 1 shows the conceptual drawing of the proposed devices.

Critically ill patients require continuous temperature monitoring and many parameters that determine biosensor performance are highly temperature dependent. These two issues validate the incorporation of a temperature sensor in microcatheters. Diseases such as hyperthrombotic states and atherosclerosis alter the blood flow, thus differing blood flow profiles can be monitored by incorporating a flow sensor into microcatheters. Additionally, real-time continuous *in vivo* glucose monitoring is required in patients with critical illness. By integrating additional microsensors into catheters using our new fabrication process and sensor configurations, we will facilitate better real time diagnostics and therapy.

2 Design and fabrication

Due to limitations in cleanroom fabrication methods, it is difficult to develop microsensors on the flexible substrates larger than 3 in. As a result, in this work we developed approximately 0.5~1 cm long spirally rolled polymer tubes with embedded microsensors and integrated the device into a commercial catheter tip (Silastic Laboratory Tubing; ID= 0.64 mm, OD=1.19 mm). Spirally-rolled polymer tubes with integrated temperature, flow rate, and glucose sensors outside the tube were fabricated using standard BioMEMS

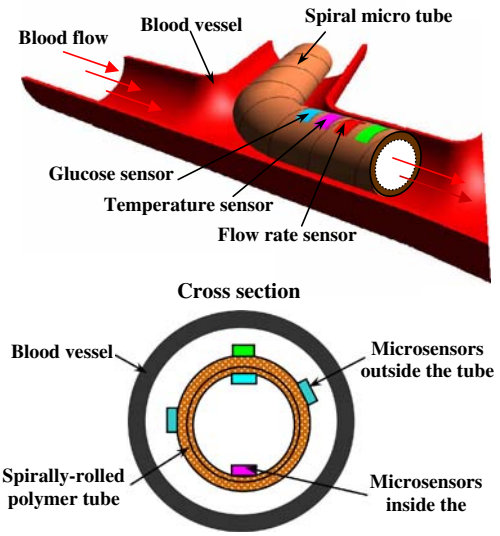

Fig. 1 Conceptual drawing of a complex sensor module for smart micro catheter. Microsensors can be fabricated inside and/or outside of the polymer tube which is impossible to fabricate with conventional packaging technologies and no micromachining technologies are available

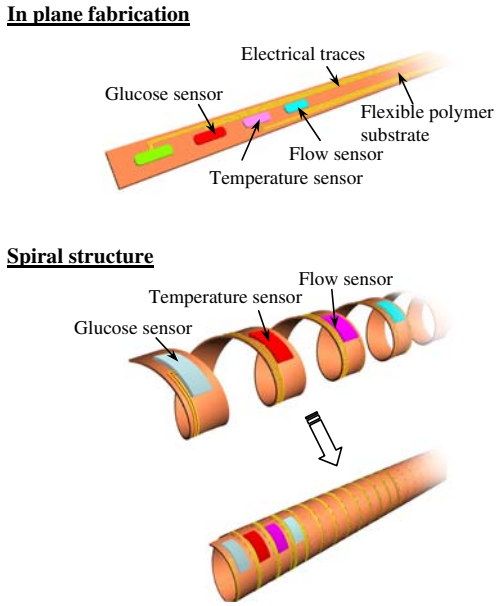

Fig. 2 Illustration of the proof-of-concept the spiral microstructure with integrated temperature, flow and glucose sensors fabricated from standard planar processes

techniques. Figure 2 illustrates the basic principle of spiral microstructure formation from planar process. It consists of two steps; fabrication of microsensors and spirally rolling the flexible substrate with sensors to make a tube structure. In this work, we demonstrated our new idea by fabricating microsensors with well-known operating principles.

2.1 Theoretical background

The working principles of fabricated microsensors outside the spirally rolled polymer tube are illustrated in Fig. 3. The advantages of using Kapton film (25 μm thickness) as a substrate to fabricate these sensors are: (a) it allows good flexibility, mechanical robustness, biocompatibility and low material cost; (b) the film has a very low thermal conductivity, thus reducing thermal losses caused by conduction, achieving lower power consumption to avoid heating fluid flowing over the sensor, and ultimately obtaining faster and more accurate measurements and (c) it provides unique advantages in terms of immunity to motion artifacts for biosensor fabrication.

A resistance temperature detector (RTD) is basically a temperature sensitive resistor. If the TCR (temperature coefficient of resistance), α, is independent of temperature, the relationship between resistance and temperature of the material can be written as

$$R(T) = R(T_0)(1 + \alpha(T - T_0))$$

Where T_0 is the room temperature. If a constant current is applied, the voltages measured across the RTD should be different at different temperatures.

Flow sensors use the well characterized principle of hot film anemometry and are operated in constant temperature mode. The sensor is incorporated into one arm of a Wheatstone bridge and heated by an electrical current. When fluid flows over the sensor, it convects heat away from the RTD, but the imbalance of the bridge causes the current to increase through the RTD, heating it to keep constant temperature. The bridge voltage represents the heat transfer and is thus a direct measure of the velocity of flow. The sensitivity of the sensor, denoted S_v, is the ratio between the changes in output voltage (V) and changes in flow rate (Q), i.e.

$$S_v = \frac{\Delta V}{\Delta Q}$$

Many micro glucose biosensors have been intensively investigated. The majority of glucose sensors are based on amperometric detection and there is considerable interest in the development of glucose biosensors that involve H_2O_2 quantification. The main principle for these glucose sensors is based on electrochemical detection of H_2O_2 produced in the following enzymatic reaction.

$$\text{Glucose} + O_2 + H_2O \xrightarrow{\text{Gox}} \text{Gluconolactone} + H_2O_2$$

$$H_2O_2 \rightarrow O_2 + 2H^+ + 2e^-$$

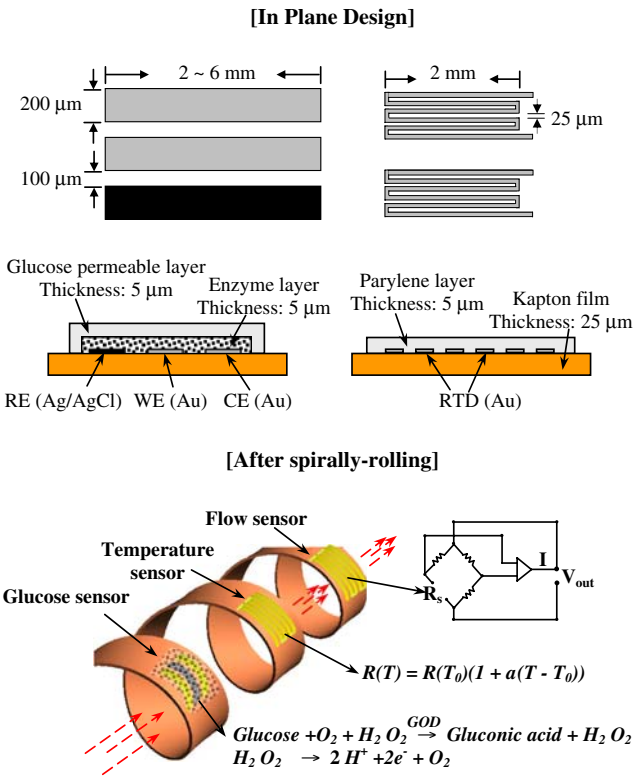

Fig. 3 Design and working principle of glucose biosensor (enzyme based amperometric detection), temperature sensor (*RTD*) and flow sensor (hot film anemometry) in spirally rolled configuration

The current resulting from the reaction is measured and is proportional to the glucose concentration in the sample.

2.2 In-plane fabrication

Polydimethylsiloxane (PDMS, Sylgard 184A and 184B) was spin-coated onto a Silicon wafer and cured at 70°C in an oven for one hour. A Kapton film (Dupont 100 HN) was cleaned and treated with oxygen plasma before it was attached to the PDMS surface and vacuumed to remove bubbles trapped between two layers. In this way, a very flat surface was achieved and the bond strength between Kapton film and PDMS was strong enough to withstand all microfabrication process steps while remaining weak enough for removal of the Kapton film from PDMS surface after fabrication. Microelectrodes were fabricated by standard thin film deposition/patterning and photolithographic techniques. The electrodes for glucose sensors and metal patterns for temperature and flow rate sensors were fabricated by depositing and patterning a Au (1,000 Å) layer with an adhesion layer of Ti (100 Å) on the 25 μm Kapton substrate using an E-beam evaporation process, followed by a standard lithography and etching processes. One of the Ti/Au electrodes was selectively electroplated with Ag as a reference electrode and chloridized by reverse electroplating in 1 M KCl solution so that Ag/AgCl reference electrode was formed. An enzyme matrix and semi-permeable membrane for the glucose sensor were then screen-printed. Enzyme matrix solutions were made according to the work reported by Gao (Gao et al. 2002, 2003), in which glucose oxidase was immobilized by using polyacrylamide solution. As a semi-permeable membrane, to enhance the stability and adhesion between the protective membrane and the enzyme layer and also firmly fix the enzyme membrane and avoid mechanical peeling stresses caused by bending, 2% (*w*/*v*) epoxy–polyurethane THF solution containing about 30% epoxy adhesive and curing agent and about 70% poly urethane (wt.) reported by Yu et al. (2005, 2006) was screen printed on top of the enzyme membrane and around edges. All the electrodes and leads were encapsulated by 5 μm thick Parylene coating to achieve electrical insulation and good biocompatibility. Finally, the entire Kapton film was removed from the PDMS layer and cut to size for subsequent spiral rolling.

2.3 Spiral-rolling

Polymer tubes can be fabricated by rolling flexible polymer strips such that adjacent regions overlap with gaps or without gaps. In this work, a smooth inner tube wall was obtained by spirally rolling the Kapton strip without gaps as shown in Fig. 4. The spiral rolling process was accomplished by using a high precision lathe (Precision Micro-Fab), film holders and power supply as indicated in our previous work (Li et al. 2005a, b).

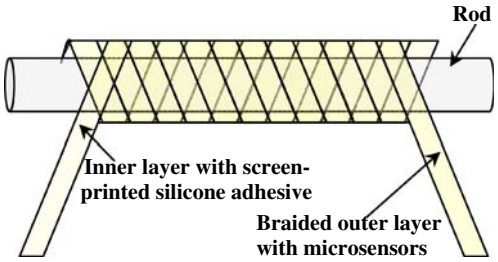

Fig. 4 Spirally rolling process: Functional Kapton film with screen-printed silicone adhesive is wrapped first. Then, followed by wrapping of Kapton film with embedded microsensors in this application

Geometric relationship for the spirally rolled polymer tube is tube inner diameter (D), film width (W) and spiral wind angle (θ). It was determined by a relationship as presented:

$$\cos\theta = \frac{\mathrm{W}}{\Pi \cdot \mathrm{D}}$$

Using this relationship several parameters can be adjusted while maintaining a constant tube diameter. Focusing on the sensor dimensions, we fixed the polymer strip width as 1 mm and changed the wind angle for different diameter polymer tubes. After spirally rolling the first Kapton strip with screen-printed implantable grade silicone adhesive (MED ADH 4100 RTV), the second Kapton strip containing embedded microsensors was spirally rolled using the same method but with opposite spiral direction. When these two Kapton strips are adhered together, a stable and strong braided structure results. A fabricated spirally rolled polymer tube with temperature, flow rate and glucose microsensors inside is shown in Fig. 5.

3 Experimental results and discussion

3.1 Flexibility test

To test the flexibility of the polymer tube, we defined that the spirally rolled polymer tube consists of three layers: outer unit, elastic adhesive layer and inner unit. One unit consists of three loops and it is bent through a certain fixed curvature. The bending model of one unit of the flexible polymer tube is shown in Fig. 6(a). When the tube starts to be bent, the inner unit starts to be bent first, then followed by the adhesive layer and outer unit. In this work, we defined the maximum bending angle as the point when the inner unit reaches the maximum bending point and starts to kink. Many parameters affect the bending angle α, such as the width of the polymer strip W, the thickness of the polymer strip T, the thickness of the adhesive layer δ, the gap between each loop g, the tube diameter D and the spiral

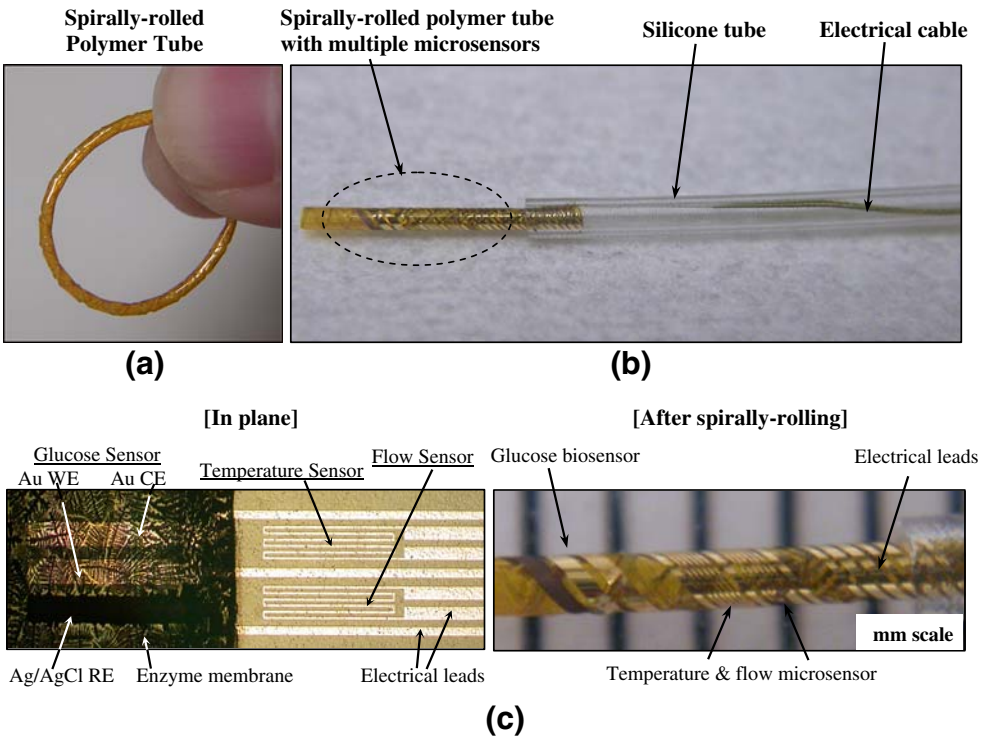

Fig. 5 Photograph of the fabricated devices: (**a**) spirally rolled Kapton tube which shows enough flexibility to travel through high curvature sections, (**b**) assembled spirally rolled Kapton tube (ID=500 μm, OD=650 μm) with microsensors outside into Silastic Laboratory Tubing (ID=0.64 mm, OD=1.19 mm) and (**c**) in plane and spirally rolled structure of glucose, temperature and flow microsensor

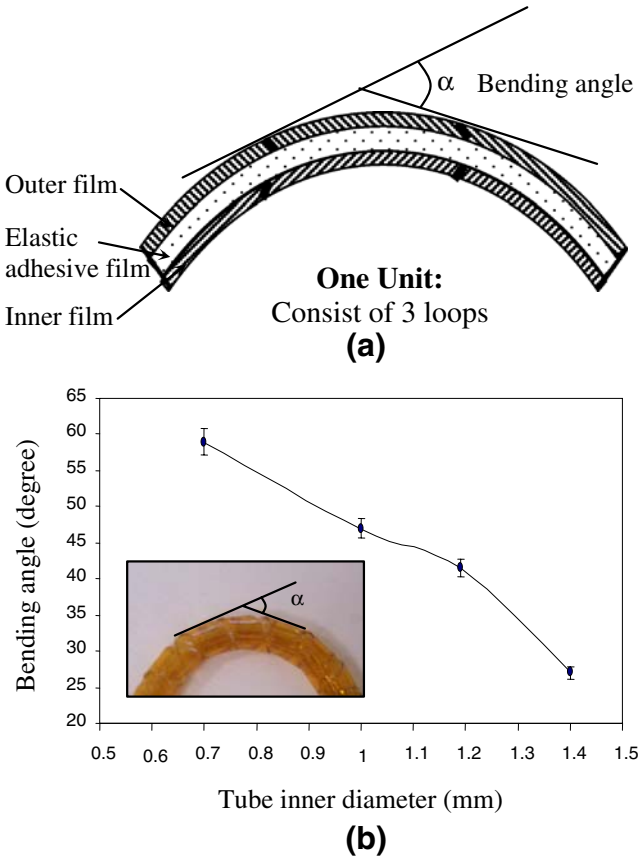

Fig. 6 Flexibility test: (**a**) bending model of one-unit and (**b**) measured maximum bending angle of the one unit. The bending angles were recorded when the inner unit starts to be kink

wind angle θ. To simplify the test, we fixed the width of the polymer strip as 1 mm, the thickness of the silicone adhesive layer as 40 μm and the gap between each loop as 0. Figure 6(b) shows that decreasing the diameter of the polymer tube results in an increase in the bending angle. The maximum bending angle of one unit is approximately 58° for the flexible polymer tube with its diameter of 700 μm. If the device is to be placed in the catheter, it is expected that the bending and stresses on the sensors may change significantly as it is used in the body, so it may affect the sensor responses. Comparing with the approach of directly assembling microsensors on the flexible substrates, which also keeps the catheter flexibility and lumen potency, this spirally rolled tube-type platform has the advantage of providing much more space to assemble more of the required sensors due to larger surface areas. Additionally, this method prevents the flexible microsensors from bending because within the tube maximum bending range only the elastic silicone adhesive layer is bent, thus the microsensors embedded in the tube wall keep the same curvature.

3.2 Leakage test

Leakage tests were performed to characterize the seal of the braided spirally rolled polymer tubes using implantable grade silicone adhesive. One outlet of the spirally rolled polymer tube is coupled with a pressure transducer and a syringe by a three-way connector. The other outlet port of

the polymer tube was sealed by two parts instant epoxy. The pressure in the tube is steadily increased by depressing the syringe cylinder, and both the volume and the pressure were recorded by LabView Program. The pressure is proportional to the reciprocal of the enclosed volume of the polymer tube in the test pressure range and can be predicted by the ideal gas law,

$$P \cdot V = n \cdot R \cdot T$$

where P is the pressure, V is the volume, n is the mole number, R is the universal gas constant, and T is the temperature. The linear response between the pressure and the enclosed volume shown in Fig. 7(a) implies zero leakage up to the maximum test pressure, 110 kPa.

Another liquid leakage test was performed to characterize the seal of the spirally rolled polymer tubes for drug delivery application. The leakage test was conducted by connecting a syringe pump via one silicone tube to a spirally rolled tube. We used phenolphthalein, a pH indicator that changes color from colorless (transparent) to red for pH values greater than eight, which is commonly used to evaluate mixing on the microscale (Kim et al. 2005) and macroscale (Zhang et al. 1995), to evaluate very small leakage of the tube by observing color variations. The spirally rolled tube was immersed into the 0.31 mol l^{-1} phenolphthalein in 99% ethyl alcohol solution bath, which was separated into two layers with a plastic plate with two holes. A solution containing 0.33 mol l^{-1} NaOH in 99% ethyl alcohol, which gives a pH of approximately 13, was then injected into the spirally rolled polymer tube through the silicone tube with volumetric flow rates from 1 μl/min to 10 ml/min by a Havard Apparatus–Pump 33 syringe pump. The high concentration of NaOH was used to obtain a large color change in the phenolphthalein even with small leakage. Figure 7(b) shows the experimental results. The results show that varying the injection flow rate from low (1 μl/min) to high (10 ml/min) showed no color changes along the bent tube, demonstrating excellent sealing and no leakage at the polymer tube.

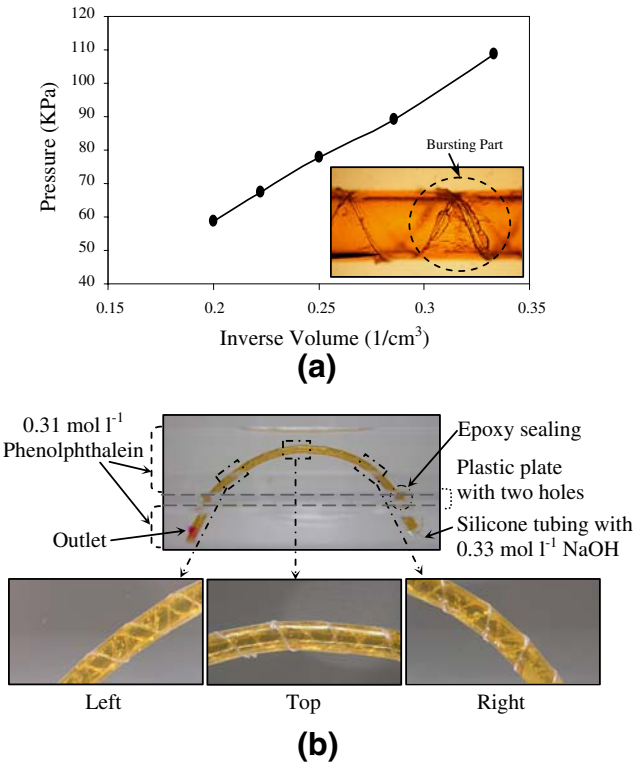

Fig. 7 Leakage test results: (**a**) Tube bursting test: graph of the pressure vs. the reciprocal of the enclosed volume of the polymer tube and (**b**) Spirally rolled polymer tube was immersed into the 0.3 mol l^{-1} phenolphthalein solution bath and 0.33 mol l^{-1} NaOH solution was injected into the spirally rolled tube with flow rate from 1 μl/min to 10 ml/min. A color change is only observed at the outlet port of the tube

3.3 Ti/Au RTD

The temperature coefficient of resistance (TCR) of the Ti/Au film was obtained by measuring the sensing element's resistance variation while slowly changing the environmental temperature of the sensing elements. The temperature standard used was a thermistor, which was inserted inside the tube. In addition, a J-type thermocouple was taped adjacent to the RTD inside the tube and plugged into a Cole-Parmer 8980-00 temperature controller with digital display. The thermocouple was used as a confirmation of the thermistor temperature. The spirally rolled tube with thermistor, thermocouple and RTD was submerged in a PBS bath (pH=7.4), which was heated by a hot plate and the temperature was monitored by a thermometer inserted into the bath. In our experiment, we minimized the input current to the RTD by applying constant direct current (Is=1 mA) so the self-heating effect could be ignored while measuring the temperature-induced voltage drop across the RTD. The RTD circuit was a simple voltage divider.

Figure 8(a) shows the temperature dependence of the sensor resistance, and that the TCR of the Ti/Au film has very little dependence on temperature. The least-squares derived regression line shows that the TCR value of Ti/Au film derived from the fitted line is 0.003 K^{-1}. Figure 8(b) illustrates the low hysteresis and high linearity of the RTD by showing the temperature measured by the thermistor as a function of RTD resistance. The RTD demonstrated linear resistance with respect to temperature that was observed in both unrolled and spirally rolled configurations.

3.4 Flow sensor

A microfabricated hot film anemometer is employed to detect flow rate. The system is set up as a constant temperature anemometer in order to achieve very high

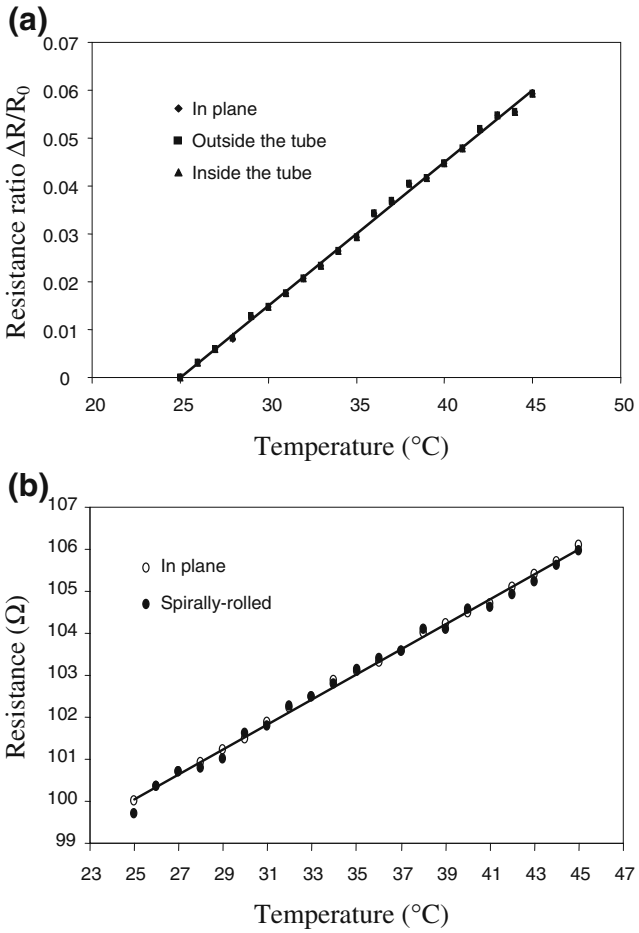

Fig. 8 Ti/Au RTD characteristic: (**a**) calculated TCR=0.003 K^{-1} at applied current I=1 mA. The value is consistent in-plane, spirally rolled outside the tube and spirally rolled inside the tube with different diameters. (**b**) RTD resistance versus the environment temperature monitored by the inserted thermocouple measured at the same time

sensitivity, low overheat ratio and short response time. The circuit that helps to monitor the temperature compensation uses the same principle as described by Ligeza (1998). The main advantage of the circuit is that the reference film can be as small as the sensor film, thus the device area can be reduced and mechanical parameters of both can be matched. The detection circuit is illustrated in Fig. 9(a). The attenuator is used to scale down the supply voltage for the half bridge comprised of the reference film. This ensures the reference film is not heated up significantly compared to the sensor film. V_{bias} serves as the startup voltage that provides the power to heat up the sensor film. The Wheatstone bridge and feedback components maintain a constant resistance of the sensor film, thus achieving constant temperature at the sensor film. It follows that the current flowing through the sensor film will vary only with changes in flow rate. Thus, one could know the flow rate by measuring the voltage at the left bridge resistance. The circuit is calibrated every time before use by subjecting the sensor film to a preset value of flow rates. Further calibration is completed by adjusting the variable resistor in the Wheatstone bridge thereby balancing the bridge. The calibration provides a reference output level under a preset flow rate so that measurement errors between each run can be minimized.

Blood constantly changes and adapts to meet the body's requirements and varies in viscosity as it flows normally. Blood viscosity also varies with disease state such as polycythemia and slightly with temperature and hence will affect the measurement of flow rate. To evaluate the effect of fluid viscosity on flow sensor performance, four different viscosity solutions, 1 cP, 3 cP, 7 cP and 93 cP were made by mixing 0% 30%, 40% and 60% sugar into PBS solution respectively. These fluids were introduced into the spirally rolled polymer tube at the flow rates from 1 to 10 ml/min using a syringe pump (Harvard Apparatus–Pump 33). Figure 9(b) shows the voltage outputs as a function of flow rate for each different viscosity fluid. The difference of flow sensor output for each different viscosity fluid at certain flow rates is smaller than 1.07%. This observation indicates that the effect of fluid viscosity on sensor performance can be ignored. A 3 mA bias current was applied with a

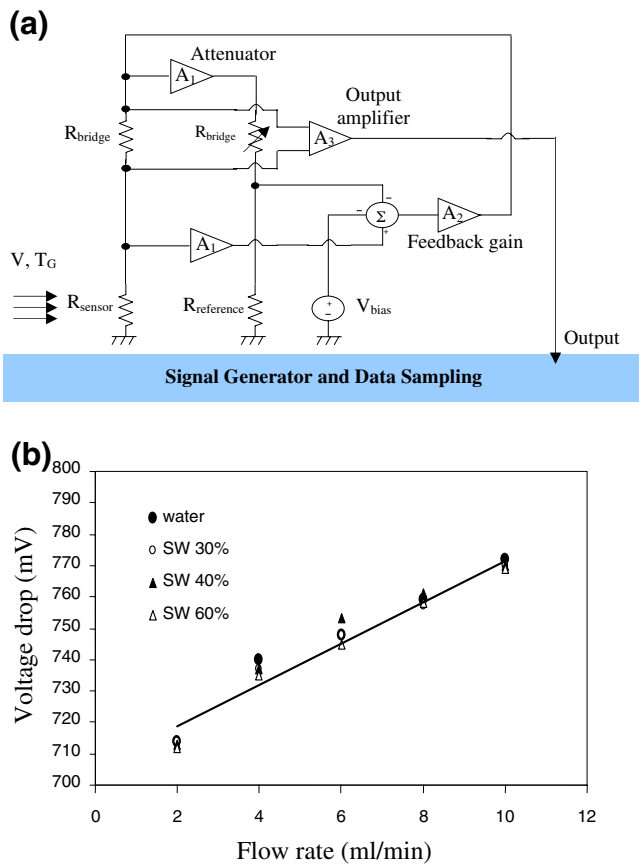

Fig. 9 Flow sensor characteristic: (**a**) detection circuit and (**b**) measurement for different viscosity sugar water (1, 3, 7 and 93 cP) at constant temperature. Sensitivity is 3.06 mV/(ml/min)

resulting sensitivity of 3.06 mV/(ml/min) and total power consumption lower than 5 mW.

3.5 Glucose biosensor

Most glucose biosensors, whether fabricated on rigid substrates or on flexible substrates (Mitsubayashi et al. 2003a, b; Kudo et al. 2006) have always had calibration plots based on data obtained from planar substrates. By rolling the glucose sensor on a flexible substrate, the solid enzyme membrane layer experiences additional stresses from changes in substrate curvature. In our previous work (Li et al. 2007), we did full characterization of the glucose biosensors in planar and rolled configurations, and observed the tendency for output signal to decrease as the tube diameter decreased (increased bending curvature). However, our rolled glucose biosensors still have adequate performance in the typical human blood range from 60 to 120 mg/dl and holds potential for improvements in the future. In this work, we focus on characterizing the glucose sensor in the rolled condition for the flexible polymer lab-chip. To check the reproducibility of the spirally rolled glucose biosensors, the output current of glucose sensors was investigated five times for each sensor and the effect of working electrode dimensions on sensor outputs was characterized. We fixed the working electrode length as 2 mm and changed the working electrode width from 200 to 600 μm. The sensor output reached a stable plateau within 50 s as shown in Fig. 10(a). An amplifying circuit that can detect as low as 1 nA was used to measure output current and the peak current values were obtained 55 s after the sample was loaded. The calibration plot for the effect of electrode area on spirally rolled glucose biosensor is shown in Fig. 10(b). As the figure indicates, the current output of the glucose sensors increase when the working electrode areas are increased. The outputs of sensors with different electrodes areas are linearly related to the concentration of glucose over a range of 20–150 mg/dl, with a correlation coefficient of 0.992 deduced by regression analysis. The sensors reproducibly respond in a linear range independently of the working electrode areas under rolled substrate conditions.

Glucose biosensors are very sensitive to temperature due to the temperature dependency of chemical reaction rate, electron mobility, enzyme activity and diffusion rate. Furthermore, there are differences between calibration temperature (room temperature), working temperature (body temperature) and the patients' body temperature. To minimize the temperature effect on sensor performance, a calibration buffer technique (Gao et al. 2003) was developed, but this technique is not practical for *in vivo* application. Integrated temperature sensors are advantageous in this case and we can obtain accurate sensor outputs by monitoring the environmental temperature simultaneously. The glucose sensor and temperature sensor performances under different temperatures were recorded simultaneously as shown in Fig. 10(c). A significant temperature dependence was

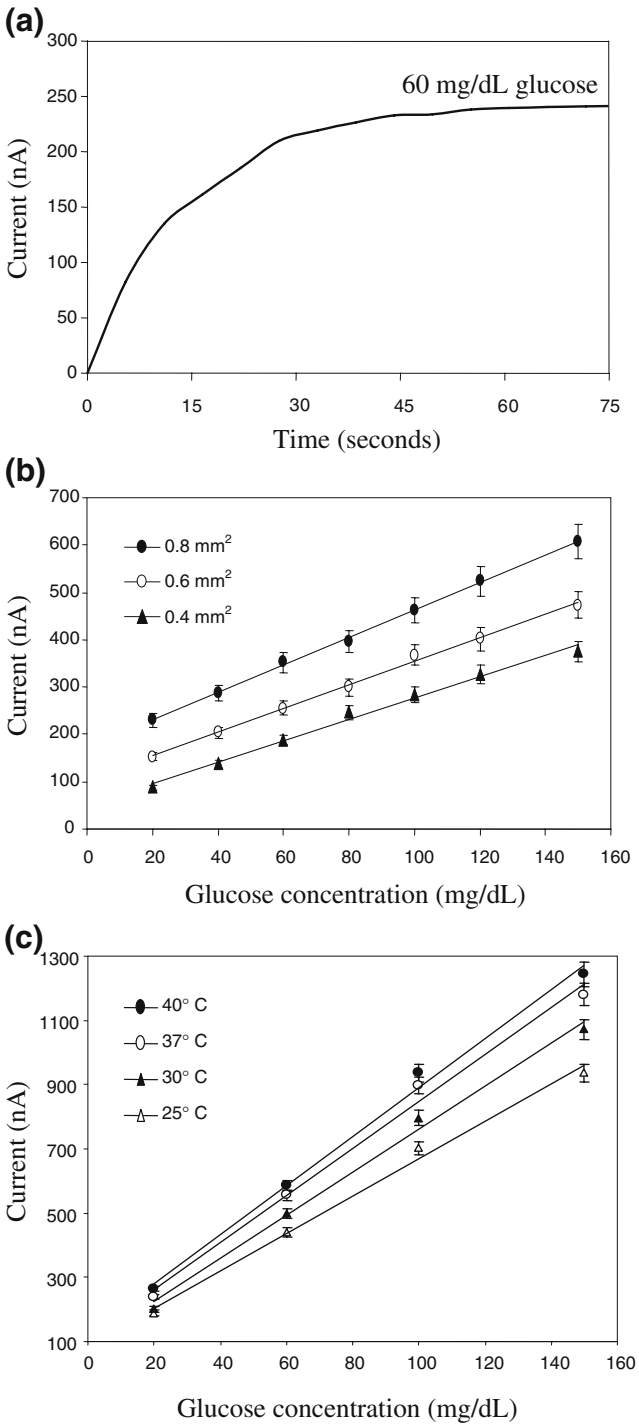

Fig. 10 Spirally-rolled glucose biosensor characteristic: (**a**) calibration curve of steady state current versus glucose concentration, (**b**) measured peak current versus different glucose concentrations for different working electrode areas at spirally rolled condition and (**c**) measured peak current versus different glucose concentrations at different temperature for the tube with OD

observed in which the current at certain concentrations increased with increasing temperature, but did not affect the glucose sensor measurement.

4 Conclusion

In this work, a novel flexible polymer tube lab-chip concept has been proposed and applied for developing smart microcatheter. As proof-of-concept, temperature, flow rate and glucose microsensors were successfully fabricated and integrated on the 25 μm thick Kapton film and then spirally rolled into different diameter tubes, followed by complete characterization. The spirally rolled microsensors have good performances in the range of normal cardiovascular catheterization and an integrated RTD can minimize the measurement error of glucose sensors due to varying body temperatures. The braided spiral structure provides good flexural rigidity and is highly kink resistant for cardiovascular catheterization. This structure also prevents the flexible microsensors from bending or being stressed outside its maximum bending range, which can affect the sensor response, thus improving results relative to the approach of directly assembling flexible sensors. As described, the fabrication process is very simple with resulting microsensors inside and/or outside the tube and suitable for low cost mass production. In addition, other MEMS components such as flexible microfluidic devices can also be integrated both inside and outside the tube, so this new spirally rolled polymer tube-type platform shows the potential of development of flexible polymer lab-on-a-tube and may open up numerous applications in other fields.

Acknowledgments This work has been partially supported from NSF-P291-L856 project. The authors gratefully thank Mr. Andrew Browne and Dr. Jaephil Do at the University of Cincinnati for their technical assistance and valuable discussion.

References

P.J. French, D. tanase, J.F.L. Goosen, Sensors for catheter applications Sen. Updat. **13**, 107–153 (2003)

C. Gao, J.W. Choi, M. Dutta, S. Chilukuru, J.H. Nevin, J.Y. Lee, P. Bissel, C.H. Ahn, A fully integrated biosensor array for measurement of metabolic parameters in human blood. Proceedings of 2nd Annual International IEEE-EMBS Special Topic Conference of Microtechnologies in Medicine & Biology (Madison, USA, 2002), pp. 223–226

C. Gao, X. Zhu, M. Dutta, S. Chilukuru, J.H. Nevin, J.W. Choi, C.H. Ahn, Development of inexpensive biosensor array for point-of-care testing. Proceedings of Micro Total Analysis Systems 2003 (μTAS2003) (Squaw Valley, USA, 2003), pp. 797–800

J.F.L. Goosen, Design considerations for silicon sensors for use in catheters and guide wires Smart Mater. Struct. **11**, 804–812 (2002)

J.F.L. Goosen, P.J. French, Integrated multiple blood parameter sensor for use in a catheter, Proc. SMIT/CIMIT (Boston, USA, 1999), p L/T-06

J.F.L. Goosen, P.J. French, P.M. Sarro, Pressure and flow sensor for use in catheters SPIE **3876**, 38–45 (1999)

J.F.L. Goosen, P.J. French, P.M. Sarro, Pressure, flow and oxygen saturation sensors on one chip for use in catheters. Proc. MEMS (Miyaaki, Japan, 2000) pp. 537–540

Y. Haga, M. Esashi, Biomedical microsystems for minimally invasive diagnosis and treatment Proc. IEEE **92**, 98–114 (2004)

D.S. Kim, S.H. Lee, T.H. Kwon, C.H. Ahn, A serpentine laminating micromixer combining splitting/recombination and advection Lab Chip **5**, 739–747 (2005)

H. Kudo, T. Sawada, E. Kazawa, H. Yoshida, Y. Iwasaki, K. Misubayashi, A flexible and wearable glucose sensor based on functional polymers with soft-MEMS techniques Biosens. Bioelectron. **22**, 558–562 (2006)

C. Li, J. Han, C.H. Ahn, Flexible biosensors on spirally rolled micro tube for cardiovascular *in vivo* monitoring Biosens. Bioelectron. **22**, 1988–1993 (2007)

C. Li, C. Gao, J. Han, C.H. Ahn, A new spirally-rolled polymer microtube with biosensors for smart microcatheter. Proceedings of Micro Total Analysis Systems 2005 (μTAS2005) (Squaw Valley, USA, 2005a), pp. 1203–1205

C. Li, F.E. Sauser, R.G. Azizkhan, C.H. Ahn, I. Papautsky, Polymer flip-chip bonding of pressure sensors on a flexible Kapton film for neonatal catheters J. Micromechanics Microengineering **15**, 1729–1735 (2005b)

P. Ligeza, A modified temperature-compensation circuit for CTA Meas. Sci. Technol. **9**, 452–457 (1998)

K. Mitsubayashi, S. Iguchi, T. Endo, S. Tanimoto, D. Murotomi, Flexible glucose sensor with a film-type oxygen electrode by microfabrication techniques. Proceedings of Transducers'03 (Boston, USA, 2003a), pp. 1201–1204

K. Mitsubayashi, Y. Wakabayashi, S. Tanimoto, D. Murotomi, T. Endo, Optical-transparent and flexible glucose sensor with ITO electrode Biosens. Bioelectron. **19**, 67–71 (2003b)

P. Mirtaheri, T. Omtveit, T. Klotzbuecher, S. Grimmes, Martinsen, T.I. TØnnessen, Miniaturization of a biomedical gas sensor Physiol. Meas. **25**, 1511–1522 (2004)

S. Nakagawa, H. Ozasa, H. Misawa, Development of micro-wiring on the outer wall of a catheter. Proceedings of Sixth International Symposium on Micro Machine and Human Science, pp. 137–143 (1995)

B. Yu, N. Long, Y. Moussy, F. Moussy, A long-term flexible minimally-invasive implantable glucose biosensor based on an epoxy-enhanced polyurethane membrane Biosens. Bioelectron. **21**, 2275–2282 (2006)

B. Yu, Y. Moussy, F. Mousy, Lifetime improvement of glucose biosensor by epoxy-enhanced PVC membrane Electroanalysis **17**, 1771–1779 (2005)

S. Zhang, S.P. Schneider, S.H. Collicott, Quantitative molecular mixing measurements using digital processing of absorption images Exp. Fluids **19**, 319–327 (1995)